Preclinical Magnetic Resonance Fingerprinting: Taking Advantage of Inherent Resistance to Motion Artifacts

Ying Gao[1], Yong Chen[2], Dan Ma[1], Yun Jiang[1], Katherine M. Dell[3], Mitchell L. Drumm[3,4], Mark A. Griswold[1,2], Chris A. Flask[1,2], and Lan Lu[2,5]

[1]Biomedical Engineering, Case Western Reserve University, Cleveland, Ohio, United States, [2]Radiology, Case Western Reserve University, Cleveland, Ohio, United States, [3]Pediatrics, Case Western Reserve University, Cleveland, Ohio, United States, [4]Genetics, Case Western Reserve University, Cleveland, Ohio, United States, [5]Urology, Case Western Reserve University, Cleveland, Ohio, United States

Introduction: High field, preclinical magnetic resonance imaging (MRI) scanners are now commonly used to quantitatively assess disease status and efficacy of novel therapies in a wide variety of rodent models. Unfortunately, conventional MRI methods are highly susceptible to motion artifacts, especially for preclinical body imaging applications where breathholds are not possible and gating can be unreliable. We have extended the novel Magnetic Resonance Fingerprinting (MRF) methodology to preclinical MRI scanners and demonstrated its capability to simultaneously assess multiple imaging parameters with inherent resistance to respiratory motion artifacts in mice and rats.

Methods: ***Preclinical MRF Design*:** The preclinical MRF acquisition was developed from a Fast Imaging with Steady-state free Precession (FISP) acquisition and implemented on a Bruker Biospec 7T MRI scanner (Billerica, MA). A FISP acquisition was used to minimize off-resonance artifacts that are extremely problematic for high field body imaging applications.[1-3] As described in the original MRF, this preclinical implementation included *a priori* variation in both flip angle (FA: 0 – 70 degrees) and repetition time (TR: 12.0 – 25.3 ms) to acquire 600 MRF images with evolving contrast.[4] An inversion preparation was applied at the beginning of the MRF acquisition to enhance the overall T_1 contrast in the MRF-FISP images. A fully-sampled Cartesian trajectory was utilized for this initial implementation. The acquired MRF signal evolution profiles were then matched on a pixel-by-pixel basis to theoretical profiles in a precalculated dictionary with more than 19,000 entries (T_1 = 100 to 2000 ms, increment = 10 ms, 2000 to 6000 ms, increment = 500 ms; T_2 = 10 to 150 ms, increment = 2 ms, 150 to 300 ms, increment = 5 ms).

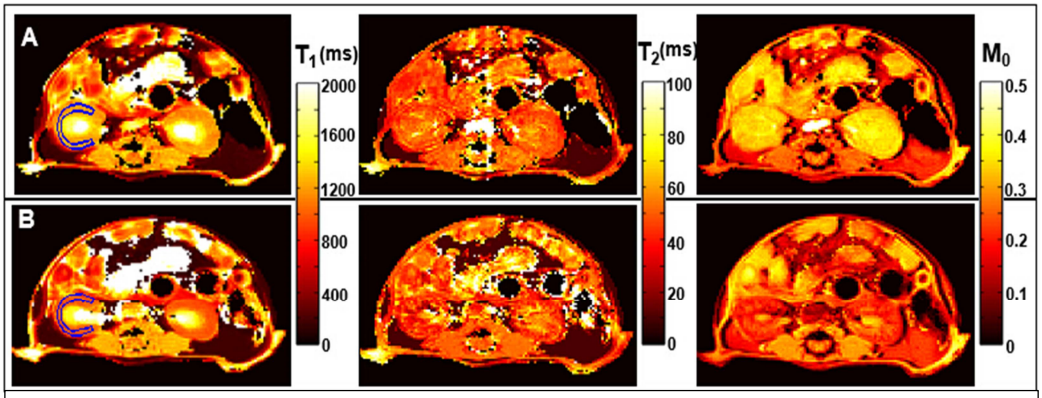

Fig.1: MRF maps from (A) *in vivo* and (B) *ex vivo* healthy mouse kidneys. Note the *in vivo* maps are devoid of respiratory motion artifacts.

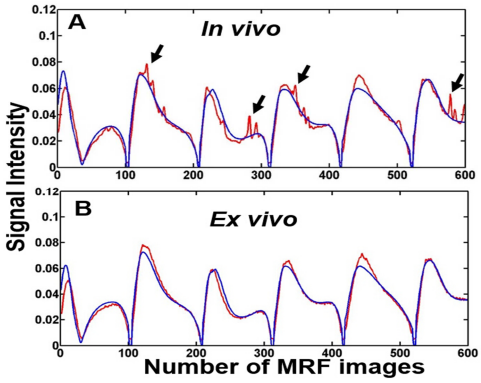

Fig. 2: Acquired (in red) and matched (in blue) MRF signal evolution profiles of mouse kidney cortex from (A) *in vivo* and (B) *ex vivo* scans. Note the overall similarity of the matched MRF profiles and resistance to respiratory motion spikes (arrows) visible in the acquired *in vivo* MRF profile, but not visible in the *ex vivo* MRF profile.

***MRF Resistance to Respiratory Motion Artifacts*:** Axial *in vivo* MRF images were acquired for healthy mouse kidneys (FOV = 3 cm × 3 cm, matrix = 128 × 128, TH = 1.5 mm, t_{acq} ~35 min). Importantly, no respiratory triggering was applied for these dynamic MRF acquisitions. Immediately following the *in vivo* MRF scans, the isoflurane concentration was increased to 5% for 30 minutes to euthanize the mouse. The MRF acquisition was then repeated on the same imaging slice to generate *ex vivo* MRF data. In a separate study, a similar MRF acquisition was also performed on a PCK rat model of Autosomal Recessive Polycystic Kidney Disease (ARPKD) to demonstrate sensitivity to known pathology.[5]

Results: *In vivo* MRF-based T_1, T_2, and M_0 maps of the healthy mouse kidneys are shown in **Fig. 1A**. Corresponding *ex vivo* images of the same slice of kidney are shown in **Figure 1B**. Reasonable T_1, T_2, and M_0 values were observed for the mouse kidneys with increased T_1 and T_2 values in the renal medulla vs. renal cortex as expected.[6] Note also the lack of respiratory motion artifacts in the *in vivo* MRF maps. Acquired (in red) and "matched" MRF signal evolution profiles from the right renal cortex are shown in **Figures 2A** and **2B** for the *in vivo* and *ex vivo* scans, respectively. Note the similar shape of the acquired MRF profiles aside from respiratory motion "spikes" for the *in vivo* MRF scan (arrows in **Fig. 2A**). Importantly, the matched MRF profile (in blue) for the *in vivo* scan ignored these respiration spikes as the motion is not encoded in the MRF dictionary. An *in vivo* MRF-based T_1 map of polycystic kidneys along with a conventional anatomic reference image are shown in **Figure 3**. The mean T_1 values of renal cysts (T_1=2420 ms) were substantially higher than that of normal renal cortex (T_1=1410 ms) as expected.

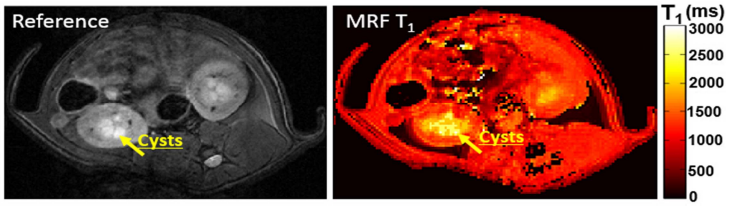

Fig. 3: *In vivo* MRF results of rat model of ARPKD.

Discussion: We have implemented an MRF-FISP acquisition on a high field small animal MRI scanner to simultaneously obtain *in vivo* T_1, T_2, and proton density maps of kidneys for both healthy mice and PCK rats. Most importantly, these results confirm that the MRF methodology is inherently resistant to respiratory motion artifacts. This feature is a key advantage for both clinical and preclinical body imaging applications where respiratory motion artifacts are particularly problematic. These results also show that our preclinical MRF technique can provide reasonable estimates of relaxation times and proton density and is sensitive to known pathology. Therefore, the MRF-FISP methodology may provide an ideal platform to assess disease progression in multiple animal models.

References: 1. Jiang Y, et al, ISMRM 2014. 2. Chen Y, et al, ISMRM 2014. 3. Gao Y, et al, NBM 2014. 4. Ma D, et al, Nature 2013. 5. Goto M, et al, JPGN 2010. 6. Nieman BJ, et al, MRM 2005.